Progress In Electromagnetics Research, Vol. 119, 207–224, 2011

AN ADVANCED DSS-SAR INSAR TERRAIN HEIGHT ESTIMATION APPROACH BASED ON BASELINE DECOUPLING

S. Li*, H. P. Xu, and L. Q. Zhang

School of Electronic and Information Engineering, Beihang University, Beijing, China

Abstract—In the distributed small satellites synthetic aperture radar (DSS-SAR), baseline is usually coupled, that is, along-track baseline and across-track baseline exist simultaneously. However, coupling baseline makes it difficult to distinguish phase differences caused by terrain height and Doppler frequency difference. In SAR interferometry (InSAR) geometric model, across-baseline is necessary to bring interferometric phase to estimate terrain height. Oppositely, along-track baseline will bring extra phase difference and dramatically decrease the accuracy of terrain height estimation. Considering the aforementioned problem, this paper focuses on the study of baseline decoupling of DSS-SAR. We firstly analyze the effect of coupling baseline on terrain height estimation, and then propose the method of baseline decoupling through space projection theory. In order to realize baseline decoupling, equivalent slave satellite, equivalent baseline, and equivalent slant range are defined through projecting slave satellite on range-height plane of master satellite. Furthermore, based on our baseline decoupling, an advanced approach of estimating terrain height is presented, which is more effective than traditional InSAR geometric model. Simulation results illuminate that the baseline decoupling can eliminate along-track baseline effect on terrain height estimation effectively and confirm the validity and efficiency of terrain height estimation approach proposed in this paper.

Received 23 April 2011, Accepted 14 July 2011, Scheduled 28 July 2011

* Corresponding author: Shuang Li (lishuang0108@ee.buaa.edu.cn).

1. INTRODUCTION

As a powerful technology to provide global high-precision digital elevation model (DEM), DSS-SAR was proposed in the end of 20th century [1]. DSS-SAR consists of several small satellites in formation flying and can simultaneously obtain SAR data of the same scene with slightly different look angle. With advantages such as small size, light weight, short development cycle, low cost and flexibility of launching and so on, DSS-SAR has evolved to an important topic of research on high resolution SAR imagery, global single-pass interferometry and ground moving target indication (GMTI) [2–4]. Moreover, DSS-SAR could overcome problems of time decorrelation and atmospheric disturbances between interferometric SAR image pair [5–7]. Especially, it can obtain dynamic baseline with large scale and flexible selection [8]. Therefore, DSS-SAR could perform well in InSAR terrain height estimation. However, DSS-SAR InSAR terrain height estimation is confronted with the challenge of coupling baseline caused by formation flying. In coupling baseline, across-baseline is necessary for InSAR terrain height estimation, while along-baseline will introduce extra phase difference into InSAR terrain height estimation [9, 10]. This paper focuses on the approach of DSS-SAR InSAR terrain height estimation based on baseline decoupling.

There are two types of InSAR terrain height estimation model for DSS-SAR, direct geolocation (DG) model and traditional InSAR geometric model [11]. They are equivalent in geolocation accuracy [12]. DG model, based on non-linear equations, are usually solved by iterative scheme and closed-form solution. It is well known that iterative scheme is prone to hypo-optimization due to observation errors of parameters and seriously depends on initial value [13, 14]. However, closed-form solution is confined with some crucial restrictions to ensure the geolocation accuracy, for example, track parallelism, track linearity and zero-Doppler processing, complicated matrix operation and additional apriori information [15, 16]. On the other hand, traditional InSAR geometric model always could obtain analytic solution with low computational burden and good robustness. Since it is proposed, it has been used more widely in InSAR terrain height estimation and its height estimation accuracy analysis, system design and performance analysis [17, 18], interferometric phase statistics characteristic analysis [19], flat earth effect derivation [20], baseline estimation [21], noise reduction and layover solution based on multi-baseline InSAR [22, 23] and so on.

Traditional InSAR geometric model mentioned in above literatures must be established in the range-height plane of master satellite.

However, as a component of coupling baseline, along-track baseline make the slave satellite out of the plane [9]. Therefore, traditional InSAR geometric model is exactly suitable to InSAR processing for DSS-SAR no longer. In order to extend traditional InSAR geometric model into DSS-SAR system, we must eliminate the effect of along-track baseline.

On the basis of baseline decoupling and traditional InSAR geometric model, an advanced DSS-SAR InSAR terrain height estimation approach is proposed in this paper. Firstly, through projecting slave satellite on the range-height plan of master satellite, baseline decoupling is performed after the phase unwrapping. It aims at eliminating the along-track baseline effect on terrain height estimation. The baseline decoupling includes three steps: calculating equivalent slave satellite to eliminate along-baseline by space projection theory; extracting equivalent baseline length and equivalent baseline obliquity from the coupling baseline; obtaining equivalent slant-range using along-track baseline. When baseline is decoupled, the traditional InSAR geometric model could be used to estimate terrain height correctly.

The reminder of the paper is organized as follows. Section 2 reviews InSAR geometric model. Section 3 analyzes the effect of coupling baseline on DSS-SAR InSAR terrain height estimation firstly. Then, the method of the baseline decoupling is presented. At last, the InSAR terrain height estimation strategy for DSS-SAR is proposed and described in detail. In Section 4, it provides the experimental result analysis to validate the InSAR terrain height estimation approach proposed for DSS-SAR. Conclusion is given in the final section.

2. INSAR GEOMETRIC MODEL

2.1. Traditional InSAR Geometric Model

The terrain height can be obtained by InSAR data, which could be acquired simultaneously (single-pass interferometry) or at different times (two-pass interferometry). Interferogram is generated by multiplying of the SAR image pair co-registered, which contains the topographic information but modulo 2π (wrapped phase). Therefore, phase unwrapping is required to recover the original phase (unwrapped phase) related to terrain height. Combining unwrapped phase and InSAR geometric model, target height can be estimated [24]. The InSAR geometric model is shown in Figure 1.

The target on the ground is defined as P. A_1 and A_2 represent the positions of the two antenna phase center respectively. B and ξ denote the length and the obliquity of baseline, which are both determined

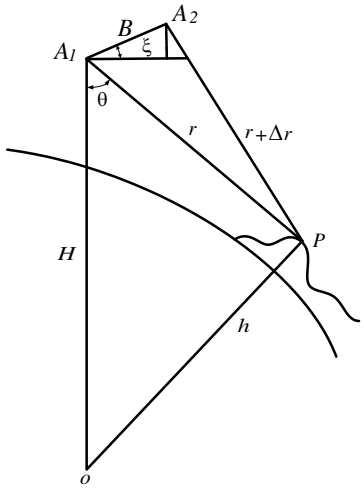

Figure 1. InSAR geometric model.

by A_1 and A_2. r represents the slant range between A_1 and target P, similarly, $r + \Delta r$ represents the slant range between A_2 and the same target. In addition, H and h are the height of satellite and target respectively. The expression of height h is given as follow:

$$h = \sqrt{H^2 + r^2 - 2Hr\cos\theta} \tag{1}$$

where, θ is the look angle and calculated by the following formulation.

$$\theta = \arcsin\left(\frac{(r+\Delta r)^2 - r^2 - B^2}{2rB}\right) + \xi \tag{2}$$

In the expression, Δr can be obtained by:.

$$\Delta r = -\frac{\lambda}{2\pi\rho}\Delta\phi \quad \rho = \begin{cases} 1 & \text{monostatic radar} \\ 2 & \text{bistatic radar} \end{cases} \tag{3}$$

where, $\Delta\phi$ is unwrapped phase.

Obviously, this InSAR geometric model is established in range-height plane of master satellite and can be applied in the system without along-track baseline effectively, such as bio-antenna system. Moreover, it is direct and convenient for accuracy analysis of height estimation, and other wide application of baseline estimation, noise reduction and layover solution based on multi-baseline InSAR and so on [13–23]. However, in the DSS-SAR system, the baseline is usually consisted of both across-track baseline and along-track baseline because of formation flying. Therefore, an advanced approach of DSS-SAR InSAR terrain height estimation is proposed in the following.

2.2. DSS-SAR InSAR Geometric Model

DSS-SAR is formation flying described by Hill's equation. Consequently, the baseline in the DSS-SAR system usually is consisted of both across-track baseline and along-track baseline. The illustration of DSS-SAR InSAR terrain height estimation is shown in Figure 2 (two satellites are exampled).

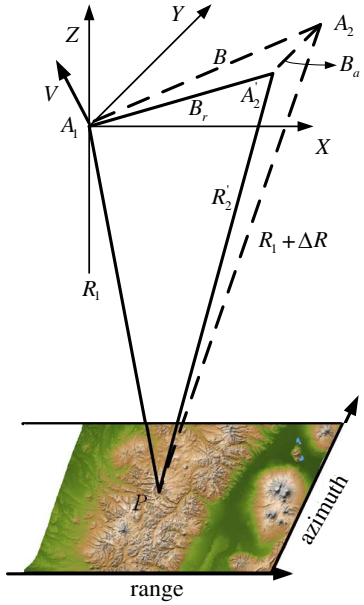

Figure 2. Illustration of DSS-SAR InSAR terrain height estimation.

In Figure 2, the target on the ground is marked as $\mathbf{P}$. $\mathbf{A_1}$ and $\mathbf{A_2}$ represent the antenna phase center of the master satellite and slave satellite respectively. $\mathbf{A_2'}$ is the projection of $\mathbf{A_2}$ on the range-height plane of $\mathbf{A_1}$. $\mathbf{B}$ is the coupling baseline determined by $\mathbf{A_1A_2}$, which can be discompose to across-baseline B_r and along-baseline B_a.

According to Figure 2, DG model consists of SAR Doppler equation and a pair of SAR range equations, and is given:

$$\begin{cases} R_1 = |\mathbf{A_1} - \mathbf{P}| \\ R_1 + \Delta R = |\mathbf{A}_2 - \mathbf{P}| \\ f_d = \dfrac{2}{\lambda R_1}\mathbf{V} \cdot (\mathbf{A_1} - \mathbf{P}) \end{cases} \tag{4}$$

where, f_d is Doppler centre frequency, λ is wavelength.

In DG model, along-track baseline and across-track baseline are coupling together. Therefore, DG model is difficult to be solved and

applied in accuracy analysis of height estimation accuracy and other extend applications list in [13–23].

3. DSS-SAR INSAR TERRAIN HEIGHT ESTIMATION BASED ON BASELINE DECOUPLING

DSS-SAR is a formation flying of small satellites that cooperate to perform the function of conventional satellite, which has the capability to implement high resolution SAR imagery, global single-pass interferometry and ground moving target indication (GMTI). In InSAR terrain height estimation, DSS-SAR is a feasible way to overcome time decorrelation and atmospheric disturbances, and obtain dynamic baseline with large scale and flexible selection. However, it is faced up to the coupling baseline. Therefore, this section will analyze the effect of along-track baseline on terrain height estimation, realize the baseline decoupling, and propose the simple and effective approach of DSS-SAR InSAR terrain height estimation based on baseline decoupling.

3.1. Along-tract Baseline Effect on DSS-SAR InSAR Terrain Height Estimation

Literature [9] has proposed that the phase difference $\phi_{i,j}$ of DSS-SAR includes two parts: one is interferometric phase ϕ_n, which is brought from the across-baseline and used to estimate terrain height; the other is azimuth phase ϕ_a which is brought from the along-track baseline. The expression of phase difference ϕ_{ij}, interferometric phase ϕ_n and azimuth phase ϕ_a are given by:

$$\begin{aligned}\phi_{i,j} &= \mathrm{mod}\left\{\frac{2\pi n_{factor}\Delta r(i,j)}{\lambda} + \frac{\pi n_{factor}\Delta f_d\,(i,j)\,x}{V}, 2\pi\right\} \\ &= \mathrm{mod}\{\phi_n + \phi_a, 2\pi\}\end{aligned} \tag{5}$$

where, interferometric phase $\phi_n = 2\pi n_{factor}\Delta r(i,j)/\lambda$ is determined by the terrain height, while azimuth phase $\phi_a = \pi n_{factor}\Delta f_d(i,j)x/V$ is determined by Doppler frequency difference $\Delta f_d(i,j)$ of complex image pair. i and j are the azimuth and range index number. mod{} is module 2π operation. n_{factor} denotes the look number.

Unfortunately, the terrain height estimation accuracy extremely depends on the precise knowledge of interferometric phase and baseline vector [25]. Therefore, in InSAR geometric model, across-baseline is necessary to bring interferometric phase to estimate terrain height, while along-track baseline will decrease the height accuracy dramatically. In order to obtain the pure interferometric phase caused

only by across-track baseline, we must eliminate the azimuth phase caused by the along-track baseline. This is the important purpose of baseline decoupling.

3.2. Baseline Decoupling

In order to estimate terrain height in DSS-SAR, baseline decoupling is proposed to eliminate azimuth phase caused by along-baseline and obtain the pure interferometric phase. The main idea of baseline decoupling is projecting the slave satellite on the range-height plan of master satellite and estimating terrain height by traditional InSAR geometric. DSS-SAR geometric model is established in the coordinates of the earth-centered fixed, and shown in Figure 3.

In Figure 3, the target on the ground is marked as **P** The velocity of master satellite is **V**. Vector $\mathbf{A}_1$ and $\mathbf{A}_2$ respectively represent the antenna phase center of the master satellite and slave satellite. Vector **B** is the coupling baseline determined by $\mathbf{A}_1\mathbf{A}_2$. R_1 and R_2 represent the slant range between the target **P** and $\mathbf{A}_1$ and $\mathbf{A}_2$ respectively. H is the height of master satellite.

According to Figure 3, baseline decoupling can be proposed by three steps: calculating equivalent slave satellite by space projection theory, extracting equivalent baseline length and equivalent baseline obliquity from the coupling baseline and obtaining equivalent slant range using along-track baseline. These steps are described in detail as following.

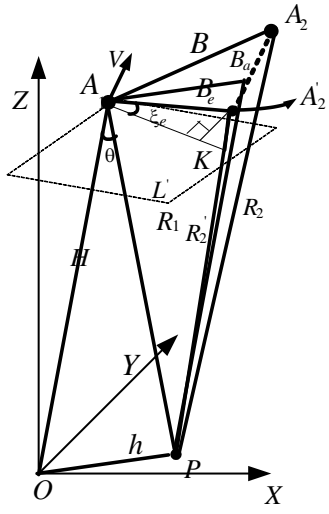

Figure 3. DSS-SAR InSAR geometric model.

3.2.1. Equivalent Slave Satellite

In Figure 3, the range-height plane of master satellite $\mathbf{A_1}$ could be represented by A_1OP. Vector $\mathbf{A'_2}$ is the projection of $\mathbf{A_2}$ on this plane, and $\mathbf{A'_2}$ is defined as the equivalent slave satellite. Equivalent slave satellite could be calculated on the range-height plane of master satellite by space projection theory.

It is assumed that $\mathbf{V} = (V_x, V_y, V_z)$, $\mathbf{A_1} = (A_{1x}, A_{1y}, A_{1z})$, $\mathbf{A_2} = (A_{2x}, A_{2y}, A_{2z})$ and $\mathbf{A'_2} = (A'_{2x}, A'_{2y}, A'_{2z})$. It is well known that vector $\mathbf{V}$ is the perpendicular direction of range-height plane A_1OP and equivalent slave satellite $\mathbf{A'_2} = (A'_{2x}, A'_{2y}, A'_{2z})$ is in the same plane. Then, the following equations can be obtained:

$$\begin{cases} V_x(A'_{2x} - A_{1x}) + V_y(A'_{2y} - A_{1y}) + V_z(A'_{2z} - A_{1z}) = 0 \\ \dfrac{A'_{2x} - A_{2x}}{V_x} = \dfrac{A'_{2y} - A_{2y}}{V_y} = \dfrac{A'_{2z} - A_{2z}}{V_z} \end{cases} \tag{6}$$

Thus, the equivalent slave satellite $\mathbf{A'_2}$ can be calculated:

$$\begin{cases} A'_{2x} = \dfrac{V_{1x}V_{1y}\left(A_{1y} - A_{2y}\right) + V_{1x}V_{1z}\left(A_{1z} - A_{2z}\right)}{V_{1x}^2 + V_{1y}^2 + V_{1z}^2} \\ \qquad\quad + \dfrac{V_{1x}^2 A_{1x} + \left(V_{1y}^2 + V_{1z}^2\right) A_{2x}}{V_{1x}^2 + V_{1y}^2 + V_{1z}^2} \\ A'_{2y} = \dfrac{V_{1y}}{V_{1x}}\left(A'_{2x} - A_{2x}\right) + A_{2y} \\ A'_{2z} = \dfrac{V_{1z}}{V_{1x}}\left(A'_{2x} - A_{2x}\right) + A_{2z} \end{cases} \tag{7}$$

when the equivalent slave satellite is obtained, the along-baseline is eliminate from the DSS-SAR InSAR geometric model, and traditional InSAR geometric established in the range-height plane A_1OP could be employed to estimate terrain height. Therefore, the calculating of equivalent slave satellite is the key step of baseline decoupling. The next step is extracting equivalent baseline from the coupling baseline, which is done in the range-height plane A_1OP as well.

3.2.2. Equivalent Baseline

In the range-height plane A_1OP, $\mathbf{A_1A'_2}$ is defined as equivalent baseline, and marked as $\mathbf{B_e}$. It is simple to calculate the equivalent baseline $\mathbf{B_e}$:

$$\mathbf{B_e} = (B_{ex}, B_{ey}, B_{ez})^T = \left(A'_{2x} - A_{1x}, A'_{2y} - A_{1y}, A'_{2z} - A_{1z}\right)^T \tag{8}$$

Equivalent baseline contains the length $|\mathbf{B_e}|$ of equivalent baseline and the obliquity ξ_e of equivalent baseline.

The equivalent baseline length $|\mathbf{B_e}|$ is given by:

$$|\mathbf{B_e}| = \sqrt{B_{ex}^2 + B_{ey}^2 + B_{ez}^2} \tag{9}$$

In the Figure 3, there must be a plane L', which is a perpendicular to the line OA_1 and ensures point A_1 in the plane. The obliquity of equivalent baseline ξ_e is the angle determined by vector $\mathbf{B_e}$ and plane L'. The plane A_1OP must intersect the plane L' at a line, at the same time, there is a point $\mathbf{K} = (K_x, K_y, K_z)$ in the line, and $\mathbf{A_2'K} \perp \mathbf{A_1K}$. Therefore, the equivalent baseline obliquity ξ_e can be expressed by:

$$\xi_e = \angle A_2' A_1 K = \arcsin\left(\frac{|A_{1x}B_{ex} + A_{1y}B_{ey} + A_{1z}B_{ez}|}{\sqrt{A_{1x}^2 + A_{1y}^2 + A_{1z}^2}\sqrt{B_{ex}^2 + B_{ey}^2 + B_{ez}^2}}\right) \tag{10}$$

After the equivalent baseline is obtained, the range between equivalent slave satellite and the target is the last parameter to be calculated for DSS-SAR InSAR terrain height estimation model.

3.2.3. Equivalent Slant Range

Equivalent slant range could be expressed by $\mathbf{A}_2'$ and the target $\mathbf{P}$, which is also in the range-height plane A_1OP and is marked as R_2'. In order to obtain R_2', along-track baseline is defined firstly. As the same as equivalent baseline, along-track baseline and its length are calculated by the following formulas:

$$\mathbf{B_a} = (B_{ax}, B_{ay}, B_{az}) = \left(A_{2x}' - A_{2x}, A_{2y}' - A_{2y}, A_{2z}' - A_{2z}\right) \tag{11}$$

$$|\mathbf{B_a}| = \sqrt{B_{ax}^2 + B_{ay}^2 + B_{az}^2} \tag{12}$$

Using $|\mathbf{B}_a|$ and R_2, equivalent slant range R_2' is calculated by:

$$\begin{cases} R_2' = \sqrt{R_2^2 - |\mathbf{B_a}|^2} \\ R_2 = R_1 + \Delta r = -\frac{\lambda}{2\pi\rho}\Delta\phi \end{cases} \tag{13}$$

where, $\Delta\phi$ is the phase different, which is the original phase obtained by InSAR data processing. Therefore, substituting the parameters $|\mathbf{B_e}|$, ξ_e and R_2' given by (9), (10) and (13) respectively into the Equations (1), (2) and (3), the terrain height could be obtained.

According to the steps above, the detailed flow chart of baseline decoupling of DSS-SAR is described in Figure 4.

After the calculation mentioned above, it can be concluded that the equivalent baseline is similar with the vertical baseline in essence.

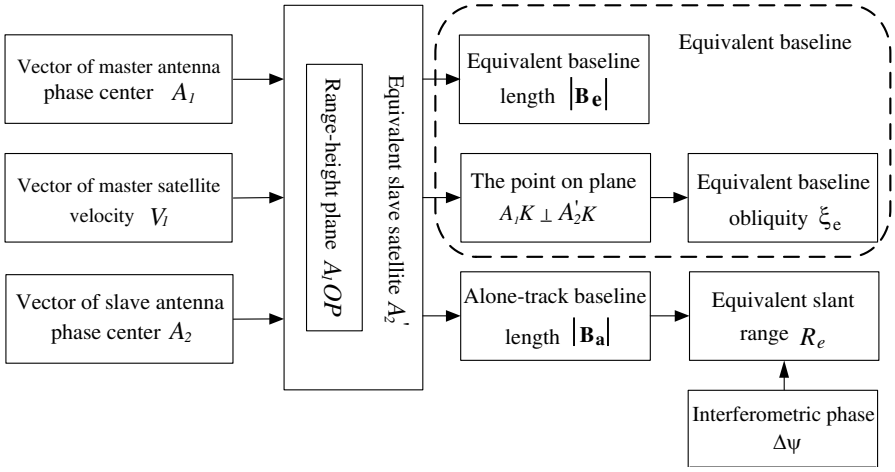

Figure 4. Baseline decoupling for DSS-SAR.

Therefore, baseline decoupling can acquire acknowledge of vertical baseline, which is widely used in InSAR system design and performance analysis. The baseline decoupling is not only benefit for DSS-SAR InSAR terrain height estimation data processing, but also DSS-SAR system design and performance analysis.

3.3. Terrain Height Estimation Based on Baseline Decoupling

Starting from the SAR single-look complex image, terrain height estimation for DSS-SAR mainly includes SAR image pair co-registration, SAR image interferometry, flat-earth phase removal, phase unwrapping, phase correction, baseline decoupling and height estimation [24, 26]. Image co-registration and phase unwrapping are the kernel steps in height estimation for DSS-SAR [27–29]. In this paper, baseline decoupling is added to data processing for DSS-SAR, which compensates the effect of along-baseline on terrain height estimation. The terrain height estimation for DSS-SAR proposed in this paper is shown in Figure 5.

Comparing the approach proposed with the flow chart of traditional InSAR data processing [24], our approach only add one step, baseline decoupling, following phase unwrapping and phase correction. Firstly, we calculate the equivalent slave satellite according to the Equations (6) and (7). Then the equivalent baseline vector could be obtained using the Equations (9) and (10). Finally, the equivalent

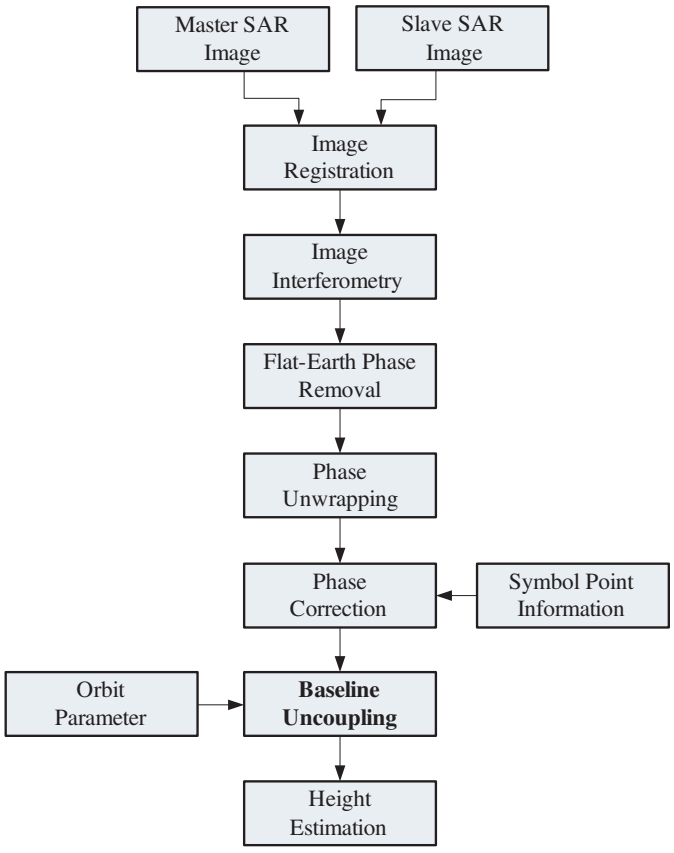

Figure 5. Flow chart of terrain height estimation for DSS-SAR.

range is derived from the Equations (12) and (13). Baseline decoupling makes coupling baseline to be projected on the range-height plane of master satellite, eliminate the along-track baseline effect on height estimation, and make traditional InSAR geometric model estimate terrain height correctly for DSS-SAR. Moreover, it permits existing techniques of InSAR data processing to be used continuously [16–23].

In this section, the paper analyzes the effect of coupling baseline on terrain height estimation, presents the method of baseline decoupling, and proposes an advanced terrain height estimation approach based on baseline decoupling for DSS-SAR. Paper places particular emphasis on the method of baseline decoupling, whose benefit to DSS-SAR system applications is demonstrated. The performance of approach proposed will be validated in the next section.

4. SIMULATION AND RESULT ANALYSIS

In simulation, formation flying of master satellite and slave satellite is designed, and orbit parameters are shown in Table 1. The radar parameters are listed in Table 2.

According to Section 3, simulation data is processed using the proposed approach. SAR single-look complex images are shown in Figures 6(a) and (b); Maximum correlation coefficient is employed in image co-registration, and SAR image co-registered is displayed in Figure 6(c). Interferogram is generated by multiplying the master SAR image with the complex conjugate of the slave SAR image, and wrapped phase is shown in Figure 6(d); Phase unwrapping is implemented through noise-immune algorithm, and unwrapped phase is shown in Figure 6(e); Symbol point information is used in phase correction, and original phase is shown in Figure 6(f); Based on baseline decoupling, terrain height is estimated, and its result is shown in Figure 6(g).

Table 1. Orbit parameters.

Parameter	Sat 1	Sat 2
Semi-major axis/m	6 886.000	6 886.000
Eccentricity	0.000	0.0007
Inclination/deg	97.000	97.000
Argument of Perigee/deg	89.000	89.000
RAAN/deg	218.000	218.000
Mean anomaly/deg	0.000	−120.000

Table 2. Radar parameters.

Item	parameter
Baseline length (3-D)	1166 m
	459 m
	330 m
Baseline Angle	20°
Platform speed	7.685 km/s
Platform Altitude	523.664 km
Carrier Frequency	9.6 GHz
Look Angle	34.36°
PRF	3200 Hz
Bandwidth	130 MHz

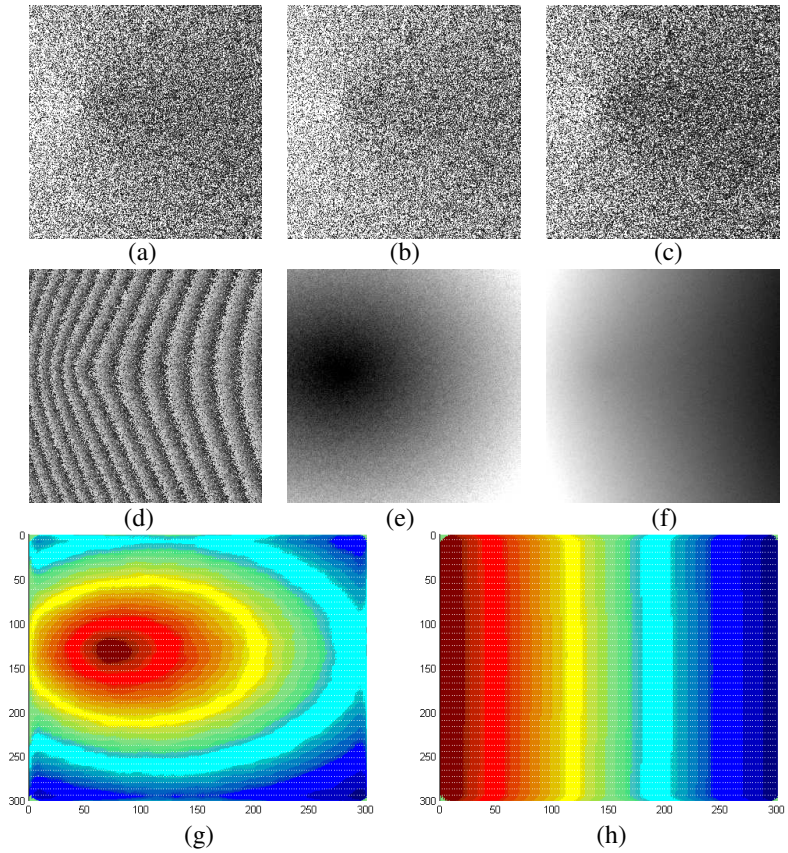

Figure 6. Simulation results. (a) Master SAR image. (b) Slave SAR image. (c) Registration SAR image. (d) Interferometric phase. (e) Unwrapped phase. (f) Original phase. (g) Terrain height estimation proposed in this paper. (h) Terrain height estimation without baseline decoupling.

Table 3. Terrain height estimation error/m.

Symbol point	Figure 6(g)	Figure 6(h)
1	1.225 6	−113.867 8
2	−0.515 5	52.725 3
3	−0.545 2	61.024 8
Relative error	1.328 2	139.454 6

The simulation of terrain height estimation without baseline decoupling is also performed, and its result is show in Figure 6(h). Table 3 indicates terrain height estimation error of the symbol point in the SAR image for the two methods.

In Table 3, terrain height estimation error of each symbol point is defined as Δh_i, and relative error is defined as Δh_r. They are calculated as following formulas.

$$\Delta h_i = h_i - \tilde{h}_i \tag{14}$$

$$\Delta h_r = \sqrt{\sum_{0<i<j<N} \left(\tilde{h}_i - \tilde{h}_j\right)^2 \Big/ C_N^2} \tag{15}$$

where, i and j are the azimuth and range index. h_i and $\tilde{h}_i$ are the theory height and estimation height of symbol points respectively. N represents the number of the symbol points.

Combining relative error listed in the Table 3 with the Figure 6(h), it is demonstrated that traditional InSAR geometric model without baseline decoupling can't obtain correct result for DSS-SAR terrain height estimation, while the approach proposed in this paper can obtain correct terrain height.

In DSS-SAR InSAR data processing for terrain height estimation, there are two main problems have to be faced up to. The first one is related to the accuracy of the terrain height estimation, and the second one is related to the method complexity.

To assess the method performances, the estimation accuracy of the method proposed in this paper can be evaluated by comparing with the CRLB in the ML case, which is used popularly [30]. The CRLB with the parameters listed in Table 1 and Table 2 is shown in Figure 7.

Figure 7 concentrates the attention on how the estimation precision changes respect to the vertical baseline. It can be concluded that the increasing of vertical baseline will lead to the decreasing of CRLB. In the Table 2, the baseline is given in 3-D coordinate. The equivalent baseline obtained through baseline decoupling is vertical baseline in actually, and its value is 500-600 m. In this case, the relative accuracy of method proposed in this paper is 1.328 2 m. The CRLB with the same parameters is 1.210424 in the ellipse shown in Figure 7. It can be seen that baseline decoupling can eliminate the effect of along-track baseline of DSS-SAR system on terrain height estimation, and is benefit to perform good accuracy for DSS-SAR InSAR terrain height estimation. Furthermore, the vertical baseline can be obtained through baseline decoupling, and it is convenient to performance analysis for DSS-SAR InSAR terrain height estimation and other applications mentioned list in [16–23].

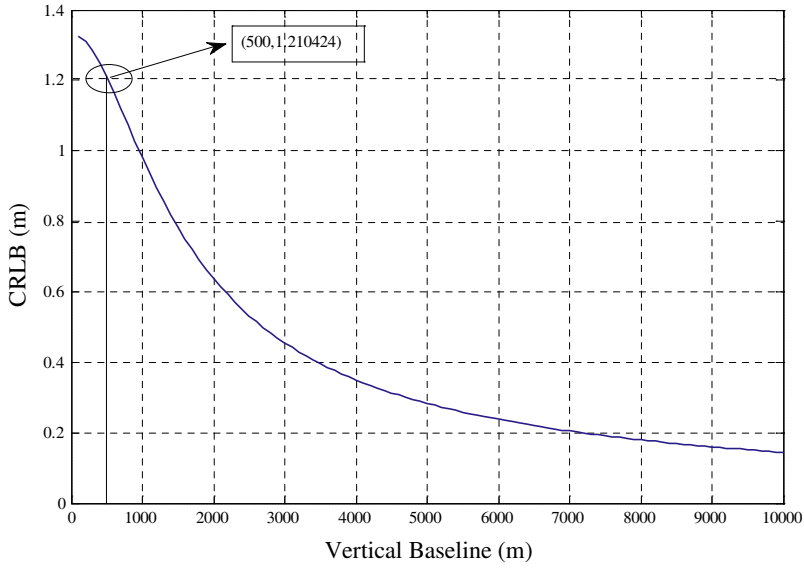

Figure 7. CRLB versus different vertical baseline.

To assess the method performances, the complexity of the method proposed in this paper can be evaluated by comparing with the DG model, which is also used popularly and has equivalent geolocation accuracy. The DG mode obtains the position of the target through solving non-linear equations, and the non-linear equations are faced up to both the uniqueness and the accuracy of the solution. It is complicated to solve. Therefore, terrain height estimation for DSS-SAR based on baseline decoupling has lower calculation burden.

5. CONCLUSION

The paper mainly discusses the advanced DSS-SAR InSAR terrain height estimation approach based on baseline decoupling. Firstly, we analyze the effect of along-track baseline on terrain height estimation for DSS-SAR. Consequently, the method of baseline decoupling is proposed, which will eliminate the along-track baseline effect aforementioned. Based on baseline decoupling, the DSS-SAR InSAR terrain height estimation approach is presented. In the end, simulation results demonstrate that the approach proposed in this paper is simple and effective. At the same time, the vertical baseline, which is obtained through baseline decoupling, is convenient to be used for system design and performance analysis for DSS-SAR InSAR terrain height

estimation. Therefore, baseline decoupling may represent a new bridge between existing techniques of terrain height estimation and DSS-SAR system.

ACKNOWLEDGMENT

The authors would like to thank all the anonymous reviewers for their careful work on this paper. This work was supported in part by the Commission on Science, Technology, and Industry for National Defense of China under Grant No. A2120060006.

REFERENCES

1. Massonnet, D., "Capabilities and limitations of the interferometric cartwheel," *IEEE Trans. Geosci. Remote Sens.*, Vol. 39, No. 3, 506–520, 2001.
2. Guo, D. M., H. P. Xu, and J. W. Li, "Extended wavenumber domain algorithm for highly squinted sliding spotlight SAR data processing," *Progress In Electromagnetics Research*, Vol. 114, 17–32, 2011.
3. Lim, S.-H., J.-H. Han, S.-Y. Kim, and N.-H. Myung, "Azimuth beam pattern synthesis for airborne SAR system optimization," *Progress In Electromagnetics Research*, Vol. 106, 295–309, 2010.
4. Mao, X. H., D. Y. Zhu, and Z. D. Zhu, "Signatures of moving target in polar format spotlight SAR image," *Progress In Electromagnetics Research*, Vol. 92, 47–64, 2009.
5. Zebker, H. A. and J. Villasenor, "Decorrelation in interferometric radar echoes," *IEEE Trans. Geosci. Remote Sens.*, Vol. 30, No. 5, 950–959, 1992.
6. Wang, T., M. Liao, and D. Perissin, "InSAR coherence-decomposition analysis," *IEEE Geosci. Remote Sens. Lett.*, Vol. 7, No. 1, 156–160, 2010.
7. Liu, D. and Y. Du, "Analysis of InSAR sensitivity to forest structure based on radar scattering model," *Progress In Electromagnetics Research*, Vol. 84, 149–171, 2008.
8. Krieger, G., H. Fiedler, and J. Mittermayer, "Analysis of multistatic configuration for spaceborne SAR interferometry," *IEE Process Radar Sonar Navig.*, Vol. 150, No. 3, 87–96, 2003.
9. Xu, H. P., Y. Q. Zhou, and C. S. Li, "Correlation of distributed small satellites SAR echoes," *Acta Electronics Sinica*, Vol. 33, No. 6, 965–969, 2005.

10. Zhu, S. Q., G. S. Liao, Z. G. Zhou, and Y. Qu, "Robust moving targets detection and velocity estimation using multi-channel and multi-look SAR images," *Signal Processing*, Vol. 90, 2009–2019, 2010.
11. Rosen, P. A., S. Hensley, and I. R. Joughin, "Synthetic aperture radar interferometry," *IEEE Proceeding*, Vol. 88, No. 3, 333–382, 2000.
12. Xu, H. and C. Kang, "Equivalence analysis of accuracy of geolocation models for spaceborne InSAR," *IEEE Trans. Geosci. Remote Sens.*, Vol. 48, No. 1, 480–490, 2010.
13. Collino, F., F. Millot, and S. Pernet, "Boundary-integral methods for iterative solution of scattering problems with variable impedance surface condition," *Progress In Electromagnetics Research*, Vol. 80, 1–28, 2008.
14. Carpentieri, B., "Fast iterative solution methods in electromagnetic scattering," *Progress In Electromagnetics Research*, Vol. 79, 151–178, 2008.
15. Nico, G., "Exact closed-form geolocation for SAR interferometry," *IEEE Trans. Geosci. Remote Sens.*, Vol. 40, No. 1, 220–228, 2002.
16. Sansosti, E., "A simple and exact solution for the interferometric and stereo SAR geolocation problem," *IEEE Trans. Geosci. Remote Sens*,. Vol. 42, No. 8, 1625–1634, 2004.
17. Rodriguez, E. and J. Martin, "Theory and design of interferometric synthetic aperture radars," *IEE Proceedings-F,* Vol. 139, No. 2, 147–159, 1992.
18. Ma, L., Z.-F. Li, and G. S. Liao, "System error analysis and calibration methods for Multi-channel SAR," *Progress In Electromagnetics Research*, Vol. 112, 309–327, 2011.
19. Just, D. and R. Bamler, "Phase statistics of interferograms with applications to synthetic aperture radar," *Applied Optics*, Vol. 33, No. 20, 4361–4368, 1994.
20. Yao, J. and D. Yi, "A concise derivation of flat earth effect and terrain height effect for across-track InSAR," *ISAPE'06*, 2007.
21. Knedlik, S. and O. Loffeld, "A new approach to improve the accuracy of baseline estimation for spaceborn radar interferometry," *IGARSS'09*, 162–165, 2009.
22. Gini, F., F. Lombardini, and M. Montanari, "Layover solution in multibaseline SAR interferometry," *IEEE Transaction on Aerospace and Electronic System*, Vol. 38, No. 4, 1344–1356, 2002.
23. Wu, B.-I., M. Yeung, Y. Hara, and J. A. Kong, "InSAR height inversion by using 3-D phase projection with multiple baselines,"

Progress In Electromagnetics Research, Vol. 91, 173–193, 2009.

24. Lanari, R. and D. Riccio, "Generation of digital elevation models by using SIR-C/X_SAR mutifrequency two-pass interferometry: The etna case study," *IEEE Trans. Geosci. Remote Sens.*, Vol. 34, No. 5, 1097–1114, 1996.
25. Xu, H., C. Kang, and Y. Q. Zhou, "The equivalent analysis of direct geocoding model and spaceborne InSAR altitude model in height uncertainty," *Journal of Electronics & Information Technology*, Vol. 32, No. 1, 48–53, 2010.
26. Zebker, H. A., T. G. Farr, R. P. Salazar, and T. H. Dixon, "Mapping the world's topography using radar interferometry: The TOPSAT mission," *Proc. IEEE*, Vol. 82, No. 12, 1774–1786, 1994.
27. Li, Z. F., Z. Bao, H. Li, and G. S. Liao, "Image autocoregistration and InSAR interferogram estimation using joint subspace projection," *IEEE Trans. Geosci. Remote Sens.*, Vol. 44, No. 2, 288–297, 2006.
28. Ghiglia, D. C. and M. D. Pritt, *Two-Dimensional Phase Unwrapping: Theory, Algorithms, and Software*, Wiley, Hoboken, NJ, 1998.
29. Li, C. and D. Y. Zhu, "A residue-pairing alogrithm for InSAR phase unwrapping," *Progress In Electromagnetics Research*, Vol. 95, 341–354, 2009.
30. Ferraiuolo, G., F. Meglio, and V. Pascazio, "DEM reconstruction accuracy in multichannel SAR interferometry," *IEEE Trans. Geosci. Remote Sens.,* Vol. 47, No. 1, 191–201, 2009.